LAMB WAVE PROPAGATION ACROSS A LAP JOINT

Zensheu Chang, Dawei Guo and Ajit K. Mal
Mechanical, Aerospace and Nuclear Engineering Department
University of California Los Angeles
Los Angeles, CA 90095-1597

INTRODUCTION

Lap joints are common elements of aircraft and other engineered structures. They are often subject to hidden defects which are caused by corrosion and fatigue, and are very difficult to detect. Development of accurate and efficient methods for the early detection of corrosion and fatigue cracks in lap joints is of considerable current interest. Ultrasonic techniques using guided waves offer the possibility of improving the technology of detecting and characterizing flaws within lap joints. It is well known that the characteristics of guided waves can be used to detect defects in plates [1]. However, the geometry of the lap joint makes it difficult to extend these techniques to lap joints. In this paper we consider the theoretical problem of the propagation of guided waves across a simple model of the lap joint in an effort to understand the interaction of the guided waves with the geometrical features of the lap joint. The geometry of the lap joint, including the vertical stress free boundaries, the rectangular corners, and the change in thickness, makes it impossible to derive a closed form solution to the problem of wave propagation across it. The problem can only be attacked by numerical methods. Conventional finite element methods fail when dealing with problems with infinite domains. In order to handle problems with local inhomogeneities or irregular shapes in an infinite domain, hybrid methods must be used.

In this paper, a hybrid method called the global local finite element method (GLFEM), first proposed by Mote [2], is used to study the characteristics of guided elastic waves propagating across the lap joint model, shown in Figure 1. The plate is separated into two overlapping semi-infinite regions containing the joint. The overlapping region is replaced by a finite element mesh, while the behavior of the waves in the semiinfinite regions is represented by Lamb wave modal expansions. Application of the continuity conditions across the mesh boundaries leads to a system of over-determined complex linear equations, which is solved by the least square method. Both the transmission and the

Review of Progress in Quantitative Nondestructive Evaluation, Vol. 15
Edited by D.O. Thompson and D.E. Chimenti, Plenum Press, New York, 1996

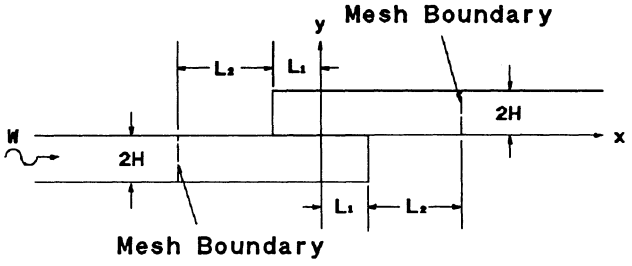

Figure 1. The geometry of the lap joint problem.

reflection coefficients are calculated and the results are checked by the principle of the conservation of energy.

METHOD

The global local finite element method can be illustrated by considering the general case shown in Figure 2, where an incident plane wave propagating in an infinite domain is scattered by an irregular-shaped inclusion perfectly bonded at the interface I. The whole domain is divided into two regions by the surface S, called the FEM mesh boundary. It should be noted that the surface S should enclose the whole inclusion. The region inside S is discretized and analyzed by the finite element method, and the behavior of the region outside S is represented by a set of global wave functions. On the mesh boundary S the displacement fields of both interior and exterior sides are forced to be the same, while the differences between the stress fields are minimized through proper choice of the amplitudes of the global functions in the sense of the least square method. The details of the method can be found in [3].

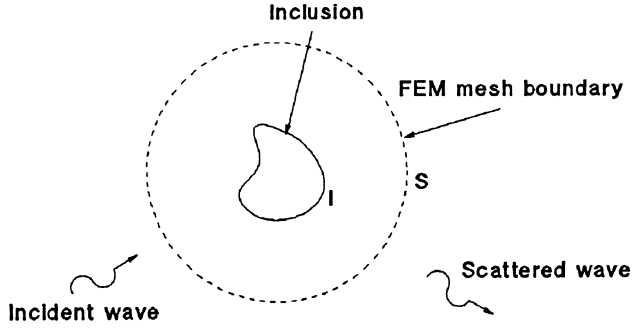

Figure 2. The general wave scattering problem in an infinite domain.

Time harmonic SH and P-SV waves propagating across a lap joint are analyzed by the method described above. The geometry of the problem is shown in Figure 1. The plate is made of aluminum, and its overlapped portion is assumed to be perfectly bonded at the interface. The guided waves are incident from the left, and are reflected and transmitted by the lap joint. The global functions used in this problem are derived from the governing equation for the time-harmonic wave in the frequency domain. The details of the derivation of the global functions can be found in the standard literature (see, e.g., Mal and Singh [4]). The results are summarized below.

SH Waves

$$w_n(x,y) = e^{ik_n x}[e^{i\nu_n y} + e^{i\nu_n(2H-y)}] \qquad n = 0,1,2,3,\cdot \tag{1}$$

where

$$\begin{aligned} \nu_n &= \frac{n\pi}{2H} \\ k_n &= \sqrt{k_s^2 - \nu_n^2} \qquad \nu_n < k_s \\ &= i\sqrt{\nu_n^2 - k_s^2} \qquad \nu_n > k_s \\ k_s &= \frac{\omega}{\beta} \cdot \end{aligned} \tag{2}$$

In Equation (2) 2H is the thickness of the plate, β is the shear wave velocity in aluminum, and k_n is the wave number of the n-th mode guided wave.

P-SV Waves - Symmetric Mode

$$\begin{aligned} U(x,y) &= [ik\cosh(\eta_1 y) - \eta_2 C\cosh(\eta_2 y)]e^{ikx} \\ V(x,y) &= [\eta_1 \sinh(\eta_1 y) + ikC\sinh(\eta_2 y)]e^{ikx} \end{aligned} \tag{3}$$

where

$$C = -\frac{(2k^2 - k_s^2)\cosh(\eta_1 H)}{2ik\eta_2\cosh(\eta_2 H)} \tag{4}$$

$$\eta_1 = \sqrt{k^2 - k_l^2}, \qquad \eta_2 = \sqrt{k^2 - k_s^2} \tag{5}$$

The associated dispersion equation is

$$\frac{\tanh(\eta_1 H)}{\tanh(\eta_2 H)} = \frac{(2k^2 - k_s^2)^2}{4k^2\eta_1\eta_2} \cdot \tag{6}$$

P-SV Waves - Anti-Symmetric Mode

$$\begin{aligned} U(x,y) &= [ik\sinh(\eta_1 y) - \eta_2 D\sinh(\eta_2 y)]e^{ikx} \\ V(x,y) &= [\eta_1\cosh(\eta_1 y) + ikD\cosh(\eta_2 y)]e^{ikx} \end{aligned} \tag{7}$$

where

$$D = -\frac{(2k^2 - k_s^2)\sinh(\eta_1 H)}{2ik\eta_2\sinh(\eta_2 H)} \tag{8}$$

The associated dispersion equation is

$$\frac{\tanh(\eta_2 H)}{\tanh(\eta_1 H)} = \frac{(2k^2 - k_s^2)^2}{4k^2\eta_1\eta_2} \cdot \tag{9}$$

The global function g_n is the vector {U,V} calculated at $k=k_n$, the n-th root of the dispersion equation, (6) or (9).

NUMERICAL RESULTS AND DISCUSSION

The hybrid method discussed above has been implemented in a FORTRAN code. The finite element mesh of the region inside the mesh boundaries is shown in Figure 3. The properties of the plate are shown in Table 1. The mesh boundary shown in Figure 1 was

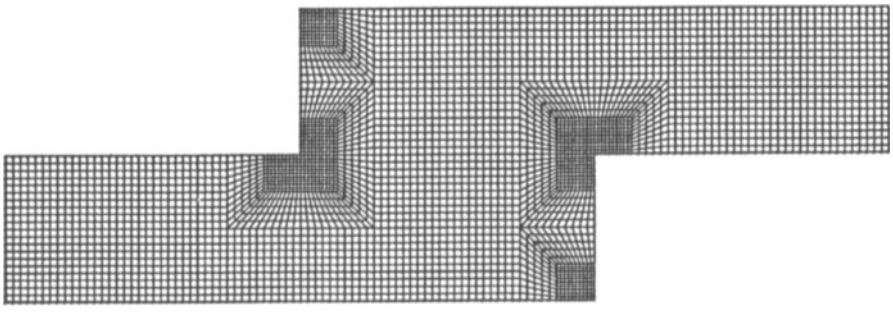

Figure 3. The finite element mesh of the lap jointed region.

Table 1. The properties of the aluminum plate used in the numerical calculations

Thickness, 2H (mm)	P-Wave Speed, c_l (m/sec)	S-Wave Speed, c_s (m/sec)	Density (kg/m^3)	Overlap Length (mm)
3.175	6.4×10^3	3.1×10^3	2.8×10^3	6.35

selected according to the following considerations. When a guided wave is scattered by a lap joint, propagating modes as well as non-propagating modes of Lamb waves are generated. The number of propagating modes at a given frequency is finite, but the number of non-propagating modes is infinite. It is impossible to include all the modes as global functions. According to Vasudevan and Mal [5], the effect of the non-propagating modes can be ignored at points about twice the plate thickness away from the wave source, which is the joint in our case. We place the mesh boundaries at a distance twice the plate thickness away from the ends of the lap joint, and use only the propagating modes as the global functions. As a result, we found that for most of the frequency sampling points, the non-propagating modes have a negligible effect outside the mesh boundary. But in certain small frequency ranges, e.g., 0.89 to 0.91 MHz, there exists one non-propagating mode which can not be ignored. This is because the decay of the mode is very slow at the specific frequency range. Of course, if we move the mesh boundary far enough away from the lap joint, this non-propagating mode may also be negligible. But this method increases the computing effort significantly. Thus instead of moving the mesh boundaries, we include the non-propagating mode as one of the global functions in the specific frequency range.

The accuracy of the numerical results is checked by the energy conservation principle. The energy flux through a vertical cross-section of the plate carried by the guided wave is calculated from the expression.

$$E_f = -\frac{\omega}{2} Im \int_S u_i \sigma_{i1}^* ds \tag{10}$$

where S is either the left or the right hand side mesh boundary. The results of the numerical method at every frequency sampling point are checked by the above formula. First, the energy flux carried by the incident wave through the left hand side mesh boundary is calculated. Then both the energy of the transmitted and the reflected waves is calculated at the right and the left hand sides of the mesh boundary, respectively. The difference between the incident and the sum of the transmitted and reflected energy is the unbalanced energy. For example, the result of the energy balance for the incident antisymmetric mode Lamb wave is shown in Figure 4. The peak of the dashed line at frequency f = 0.9 MHz, about 8 percent, is due to the exclusion of the non-propagating mode discussed above. After including the non-propagating mode, the peak is reduced to about 2 percent, as shown by the solid line.

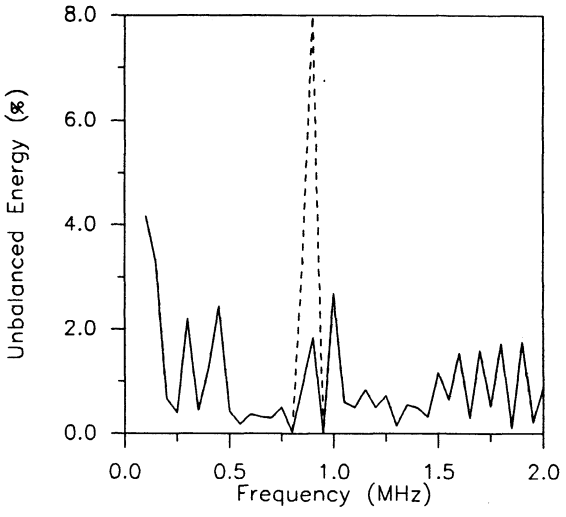

Figure 4. The unbalanced energy for incident antisymmetric Lamb wave.

At a given frequency f, the number of propagating modes depends on the value of f relative to the cut-off frequency f_n. The cut-off frequencies can be obtained by substituting the limiting value of the wave number, $k \to 0$, into the dispersion equations (e.g., Graff [6]). For the SH case, the cut-off frequencies are $f_n = nc_s / 4H$, and for the P-SV case, the cut-off frequencies are $f_n = nc_s / 4H$ or $nc_l / 4H$. For the plate of thickness 2H = 3.175 mm, the cut-off frequencies below 2 MHz are given in Table 2. It should be noted that at a specific frequency range, about 0.90 to 0.97 MHz, one of the propagating modes has a negative group velocity. The direction of the group velocity is the direction of the energy flux. In the case under investigation, there is no obstacle outside the lap joint, so there should not exist any reflected or transmitted wave carrying energy toward the lap joint. Consequently,

Table 2. The cut-off frequencies for the plate thickness 2H = 3.175 mm (MHz)
(s) : symmetric mode (a) : anti-symmetric mode

Cut-off Freq.	f_1	f_2	f_3	f_4	f_5
SH Case	0.488	0.976	1.465	1.953	
P-SV Case	0.488 (A)	0.976 (S)	1.008 (S)	1.465 (A)	1.953 (S)

the propagating mode with negative group velocity should be excluded from the global functions. Figure 5 shows how this mode affects the numerical result. The displacement amplitudes of two points on the top surface are plotted in Figure 5, the incident wave is the antisymmetric first mode of the Lamb wave. The dashed line in Figure 5 is due to the inclusion of the propagating mode with negative group velocity. After we excluded the mode, the peak disappeared as shown by the solid line. In Figure 5, the normalized displacements are the vertical displacements of the points normalized by the maximum vertical displacement of the incident wave.

In conclusion, the success of the global local finite element method depends greatly on the proper selection of the global functions. Inclusion of all the propagating modes of the Lamb wave is acceptable in most of the frequency ranges, but, at certain specific frequencies, a more detailed understanding of the features of the Lamb waves is needed in order to make the correct selection. From the energy conservation point of view the accuracy of the global local finite element method is acceptable.

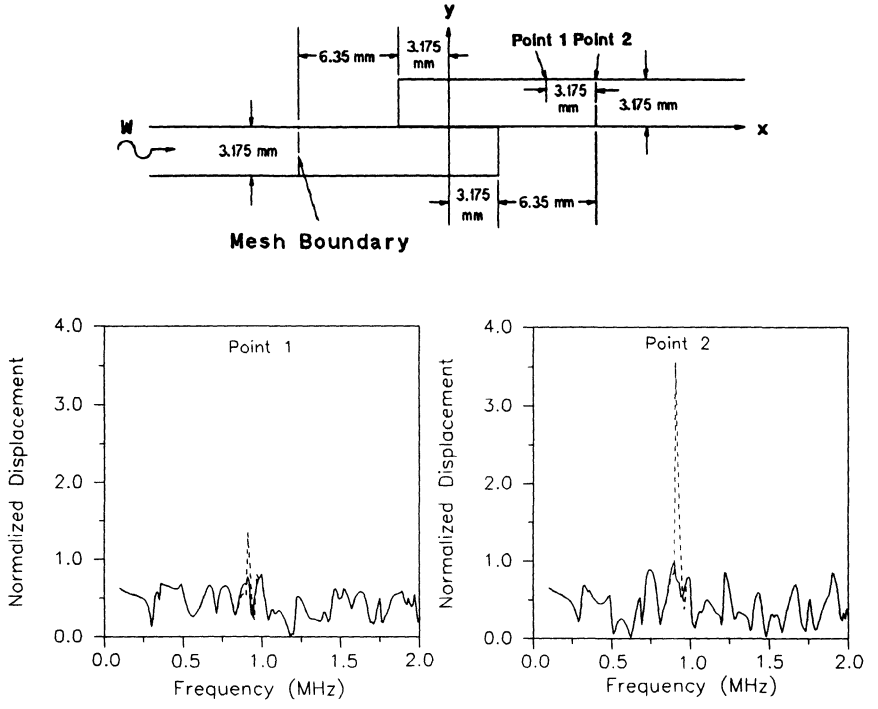

Figure 5. Displacement amplitudes at two points on the top surface for an incident antisymmetric Lamb wave. Dashed curve includes global functions with negative group velocity.

ACKNOWLEDGMENT

This research was supported by the AFOSR under grant F49620-93-1-0320 directed by Dr. Walter Jones.

REFERENCES

1. D. N. Alleyne and P. Cawley, IEEE trans. On Ultrasonics, Ferroelectrics, and Frequency Control, 39, 382 (1992).
2. C. D. Mote Jr., Intl. J. for Numerical Methods in Eng., 3, 565 (1971).
3. Z. Chang and A. K. Mal, Numerical Methods in Structural Mechanics, AMD, Vol. 204, 1 (1995).
4. A. K. Mal and S. J. Singh, Deformation of Elastic Solids (1991).
5. N. Vasudevan and A. K. Mal, J. Applied Mechanics, 52, 356 (1985).
6. F. G. Graff, Wave Motion in Elastic Solids (1975).